

Contact residual stress relaxation in soda-lime glass Part II. Aspects relating to strength recovery

K.O. Kese*, Z.C. Li, B. Bergman

Department of Materials Science and Engineering, Royal Institute of Technology, 10044 Stockholm Sweden

Received 29 August 2004; received in revised form 3 December 2004; accepted 10 December 2004

Available online 3 February 2005

Abstract

Strength recovery of Vickers indented soda lime glass was measured and compared after annealing at two temperatures: one below and one above T_g . The atomic force microscope was used to study the cracks. At 540 °C, no changes were observed in crack morphology either below the surface or on the surface relative to the pre-anneal state. At 630 °C, both sub-surface and surface crack morphology changes were observed. The trends in strength recovery were compared with residual stress relaxation as measured by a new method of stress estimation based on nanoindentation elastic response. At short hold times at 630 °C, and regardless of the length of hold time at 540 °C, strength recovery of only ~30% was measured while at moderately long hold times at 630 °C, strong recovery of fracture strength, ~132% was measured. Trends in strength recovery above T_g are shown to match those of crack tip radius instead of trends in stress relaxation across the residual stress field.

© 2005 Elsevier Ltd. All rights reserved.

Keywords: Nanoindentation; Glass; Stress relaxation

1. Introduction

Non-equal biaxial stresses are known to exist around a Vickers indent in glass. Zeng and Rowcliffe¹ used an indentation fracture method and measured tangentially directed tensile stresses and radially directed compressive stresses in the Vickers residual stress field. These stresses are high close to the edge of the indent, but decrease with distance away from it.^{2,3} Lawn et al.⁴ and Roach and Copper⁵ have determined that the residual stress field relaxes with time in humid environment. An important effect of this stress relaxation is increased fracture strength, relative to the immediate as-indented state. The reason behind the residual stress relaxation is that the tensile stress component of the stress field causes both the radial and the lateral cracks to grow during ageing.^{4–6} Salomonson and Rowcliffe⁶ found that the compressive stress component does not contribute to this post-indentation crack growth since it did not significantly change

in magnitude after a 2-month ageing period. During annealing, on other hand, Abe et al.⁷ have determined that both the tensile and compressive stress components are relaxed. The crack growth driving force of the residual stress field is characterised by the dimensionless constant, χ , and in the context of strength, applies only to the radial cracks, since the lateral cracks are passive in mode I strength testing. Thus, if the indentation produces a crack of equilibrium length, c_0 , then under the influence of the contact residual stress driving force, this crack will grow to a non-equilibrium length, c'_0 . Under an applied tensile stress, σ_a , the crack will experience a net stress intensity factor, K , given by⁸

$$K = Y\sigma_a c^{1/2} + \chi \frac{P}{c^{3/2}}, \quad (1)$$

where Y is a crack geometry factor, P is the indentation load, and c is the crack length under the applied stress. The residual stress field constant is not invariant: its value decreases as post-indentation crack growth progresses.^{6,9} For example, Salomonson et al.⁶ determined that immediately after indentation in soda lime glass with a 45 N load, the value of χ

* Corresponding author. Tel.: +46 8 790 9134; fax: +46 8 20 76 81.

E-mail address: kese@mse.kth.se (K.O. Kese).

was 0.066 but decreased, by about 32%, after crack growth saturation over 2 months to 0.045.

When the specimen is annealed it is believed that the residual stresses are completely relieved and that χ becomes equal to zero.⁸ An effect of a decreasing or zero χ is that the fracture strength, σ_f , should increase according to

$$\sigma_f = \frac{1}{Yc_f^{1/2}} \left(K_c - \frac{\chi P}{c_f^{3/2}} \right), \quad (2)$$

by rearranging Eq. (1) and setting $K = K_c$ for equilibrium conditions; c_f is the crack length at fracture. Results of previous studies^{4,5} have shown, however, that in situations where full stress relaxation is supposed to have occurred, i.e. when $\chi = 0$, full strength recovery, commensurate with the existing crack dimensions, is not achieved. Common to those studies was that the annealing temperatures were all below the glass transformation temperature, T_g , of the glass. In another study, Hrma et al.¹⁰ employed a wide range of annealing temperatures from 525 to 725 °C.

In Part I of the present study,¹¹ we introduced a new method of stress estimation based on nanoindentation elastic response, which was then used to study the isothermal annealing of the Vickers residual stress field at 540 and 630 °C. The purpose of the present paper is to closely study the strength recovery that results from isothermal annealing of the Vickers residual stress field at these two temperatures and relate it to the stress relaxation occurring across the stress field as reported in the companion paper. A special feature then with the present study is that the high spatial resolution of the nanoindentation method permits a detailed mapping of the stress relaxation across the residual stress field. This detailed knowledge of the relaxation progression across the residual stress field helps us to draw important conclusions regarding the actual role of contact residual stresses in strength recovery. For completeness, we employ the atomic force microscope and optical microscopy to study any crack morphological changes that might influence strength properties.

Crack morphological changes and strength recovery, in connection with heat treatment, is a well-studied subject.^{12–16} Thus, Lange and Gupta,¹² Yen and Cobble¹³ and Gupta^{14,15} have studied crack healing in several ceramic materials including ZnO, Al₂O₃, and MgO. There are however two important ways in which those studies differ from the present one. The first is that, apart from Yen and Cobble,¹³ crack introduction was through thermal shocking of the samples in the previous studies, which differs from the indentation induced cracks, with the associated residual stress field, studied in the present paper. The study of the relaxation of the residual stress field, and how it affect strength recovery is as important in this paper as the study of the influence of crack morphology changes on strength. The second is that, whereas crack morphology changes were followed in the previous studies until spherical pores were formed, in the present study, spheroidization was avoided since, at that stage, there is the possibility of fracture starting at flaws other than the

initial indentation site.¹⁰ Although Hrma et al.¹⁰ employed several temperatures in their study, it is important to point out that no significant strength recovery was obtained at temperatures below 600 °C in that study; when strong increase in strength occurred, it was only after a certain minimum hold time at 650 °C. The choice of the two temperatures in this paper was therefore to give a representative insight into the role of kinetics on the relaxation of the Vickers residual stress field on either side of T_g (~566 °C) and to show how this ultimately influences the strength recovery achieved in the material. A further important feature of the present study is that we have facility, through the AFM, to experimentally measure the radius of annealed cracks, thus giving us the opportunity, as will be shown, to directly relate trends in strength recovery to those in crack tip radius.

2. Experimental

Sets consisting of 18 or 9 samples of 3 mm-thick, 35 mm by 35 mm soda lime glass plates were indented, one set at a time, with a 45 N Vickers indenter, thus creating the well-known Vickers residual contact system. After indentation, each of those sets that consisted of 18 samples was divided into two equal subsets: one was immediately put in the furnace for annealing while the other half was kept in air for ageing for as long as the annealing experiment lasted. After annealing, the samples of the two subsets were strength-tested together. Therefore, at the time of strength-testing, the Vickers residual contact system in all the samples of the two subsets had had the same lifetime. Those sets that consisted of nine samples were annealed immediately after indentation as before but this time without any ageing counterparts. On fracturing the annealed samples together with their aged counterpart samples, it was found that the strength of the aged samples did not increase significantly after a certain length of ageing time. The ageing tests were therefore discontinued in some of the tests as shown by the gaps in Table 1. The annealing temperatures were 540 and 630 °C. At 540 °C, the annealing hold times were 0, 24, and 48 h whilst the hold times at 630 °C included 0, 15 min, 30 min, 2 h, 4 h, 6 h and 12 h. Table 1 shows a summary of the experimental schedule. Strength testing was done by loading the specimens in biaxial stress using the ring-on-ring method at a cross-head speed of 0.2 mm/min. The radius of the support ring, r_s , was 7 mm while that of the loading ring, r_l , was 3 mm. Fracture stress was calculated using the expression following expression⁶:

$$\sigma_f = \frac{3F}{4\pi t^2} \left[2(1 + \nu) \ln \frac{r_s}{r_l} + \frac{(1 - \nu)(r_s^2 - r_l^2)}{R^2} \right]. \quad (3)$$

F is the load at fracture; t , the thickness of the glass plate, ν , the Poisson's ratio of the sample while R is half the average length of the diagonals of the sample. The optical microscope and the AFM were used to examine the indentation site, both on the sample surface and the fracture surface, to study any

Table 1
Schedule of annealing and ageing tests

	Set 1	Set 2	Set 3	Set 4	Set 5	Set 6	Set 7	Set 8	Set 9	Set 10
Sub-set of nine samples for annealing										
Temperature (°C)	540	540	540	630	630	630	630	630	630	630
Time (h)	0	24	48	0	0.25	0.5	2	4	6	12
Sub-set of nine samples for ageing only	Yes	–	–	Yes	Yes	Yes	Yes	–	–	–

changes in the indent/crack system as a result of the annealing exercise.

3. Results and discussion

3.1. Crack studies

Table 2 summarises the crack lengths measured in this study. To determine the virgin crack length, c_0 , a set of samples was indented. In this case the cracks were measured immediately after each sample was indented, instead of measuring them after all the samples in the set had been indented. Crack lengths measured under the latter circumstance are designated c_1 in the notes under Table 2 while those measured after long time ageing are denoted by c_s . Crack growth occurred between the time of indentation and when annealing started, as a comparison between c_0 , c_1 and the crack lengths after annealing of sample sets 1–7 may show. It may be inferred from the same observation that no change in crack length occurred during annealing. This is however not true for the samples that were annealed for more than 2 h at 630 °C, where the cracks decreased in length during annealing. This was accompanied by a change in crack configuration in the surface of the specimen. The change included crack tip rounding, widening of crack opening and material pileup adjacent to the surface trace of the sides of the crack as has been reported by Hrma et al.¹⁰ Decrease in crack length especially under elevated temperature and humid conditions, has been studied extensively in the literature for glass,^{17–20} and the phenomenon has been

called crack healing. It is believed^{10,20} that viscous flow at the temperatures involved is responsible for the changes in crack morphology that are observed.

Fig. 1 shows AFM images of crack tips representing results of some of the annealing schedules employed in this study. As may be seen the cracks tips are barely resolved for specimens annealed for less than 2 h at 630 °C. The same was the situation with the specimens annealed at 540 °C. Even after 48 h annealing at that temperature the crack tip did not look different from an unannealed one, when examined with the optical microscope. Beyond 2 h at 630 °C however, the crack tip is easily resolved by the AFM. Representative crack-tip radius measured for the 630 °C tests are plotted against annealing hold time in Fig. 2, where a marked increase in crack tip radius at long (>2 h) hold times at 630 °C may be seen. Thus whereas the surface trace of the radial cracks are thin slits emanating from the corners of the indentation at short hold times at 630 °C and lower temperatures, at longer hold times at 630 °C, these are transformed into elongated elliptical apertures with rounded ends. Fig. 3 shows AFM sections of the cracks, near the tip, as a function of anneal time. At 0 and 15 min hold time the crack opening is not very different from the surface roughness of the specimen. As the time increases, the crack widens and obtains raised edges. The near-surface and surface features thus become resolvable for the AFM tip. The sub-surface depth information suggested in Fig. 3 cannot be correct for the short hold times, especially up to 2 h. It is either that the AFM tip is larger than the size of the crack opening and/or that the tip is limited in its downward reach. As time increases however, for example

Table 2
Summary of crack length results

Samples set	Annealing details		Age at fracture (h)	Crack length at fracture (μm)	
	T (°C)	Hold time (h)		Aged only	Annealed only
1	540	0	24	266.05 ± 11.91	248.79 ± 11.04
2	540	24	54	–	246.14 ± 7.66
3	540	48	120	–	245.06 ± 8.26
4	630	0	29	266.41 ± 5.84	241.93 ± 5.48
5	630	0.25	30	267.42 ± 6.99	247.04 ± 5.97
6	630	0.5	30	268.24 ± 7.78	246.77 ± 7.71
7	630	2	33.5	267.12 ± 7.56	247.00 ± 9.76
8	630	4	30	–	234.17 ± 10.42
9	630	6	38.5	–	233.97 ± 15.35
10	630	12	41	–	223.97 ± 15.35

Crack length immediately (<5 min) after indentation, $c_0 = 229.00 \pm 9.40$ μm; crack length less than 1 h after indentation, $c_1 = 247.71 \pm 7.47$ μm; saturation crack length after long time (>72 h) ageing, $c_s = 271.54 \pm 8.54$ μm.

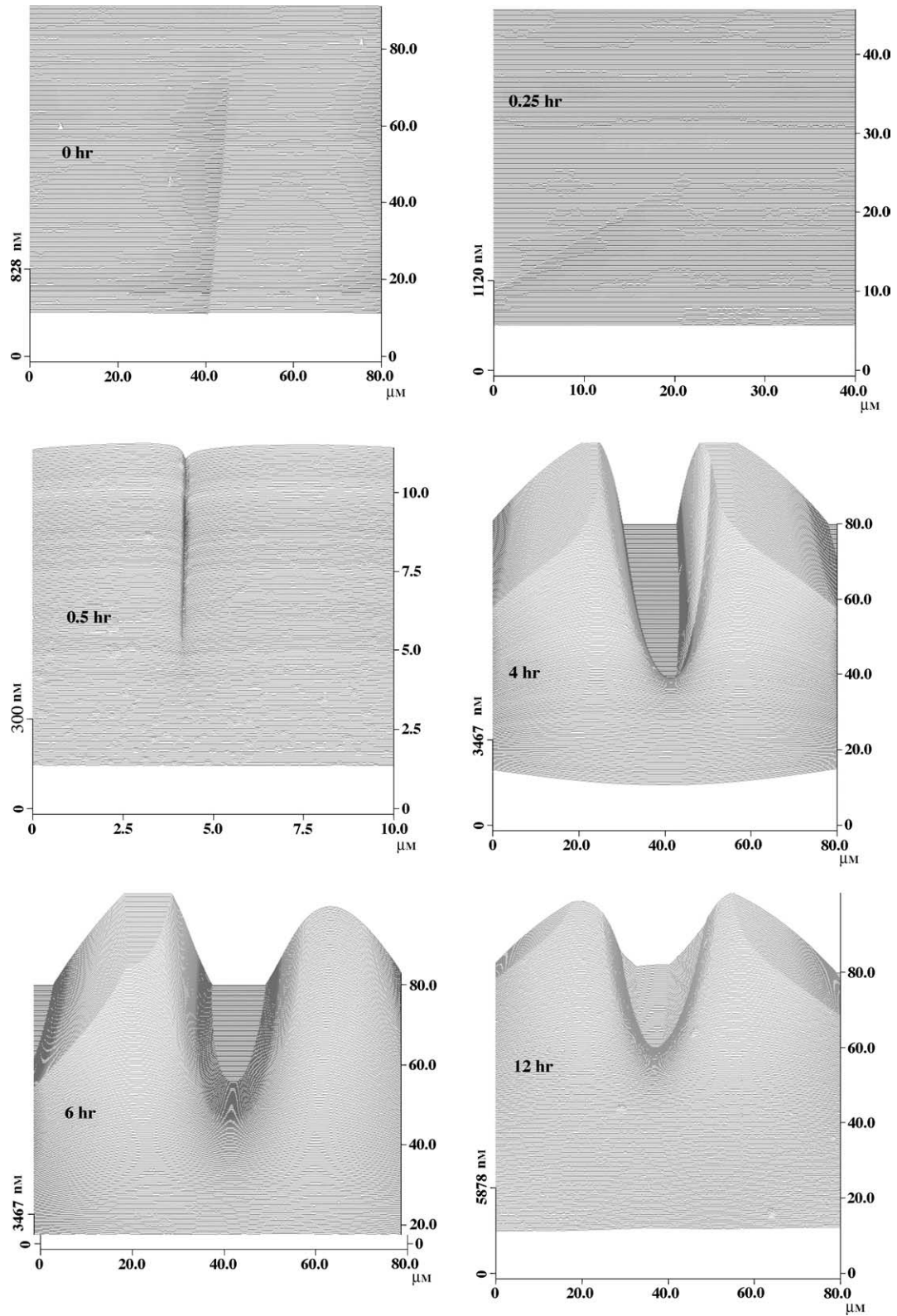


Fig. 1. 3D AFM photo sequence showing how crack tip morphology on sample surface changes with length of hold time during annealing at 630 °C.

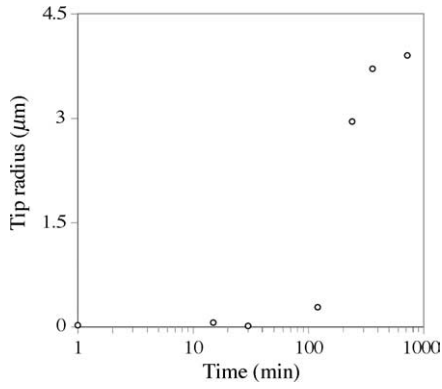


Fig. 2. Plot of crack tip radius as a function of annealing hold time at 630 °C.

for 4 h and upwards, the sub-surface situation could begin to look like what is shown in Fig. 3. When this happens, that would however not be the entire sub-surface picture since, as described in Fig. 9 of ref.,¹⁰ such a situation would be accompanied by crack bridging, whereby the surface part of the crack will be separated from the sub-surface part by a region

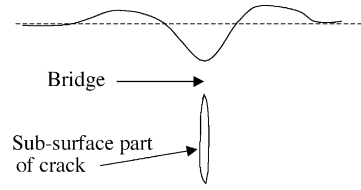


Fig. 4. Illustrating the bridge formation that separates the subsurface crack front from the surface crack.

of welded material as illustrated by Fig. 4. The width of the crack opening, the slope of the crack faces close to the zero line and the pileup dimensions, however, are accurate images of these features of the crack morphology. No crack tip radius measurements were made for the 540 °C tests since, as mentioned above, the AFM was not able to resolve the crack tips annealed at that temperature.

3.2. Strength studies

The results of the fracture strength measurements are presented in Figs. 5 and 6 for the 540 and 630 °C annealing tem-

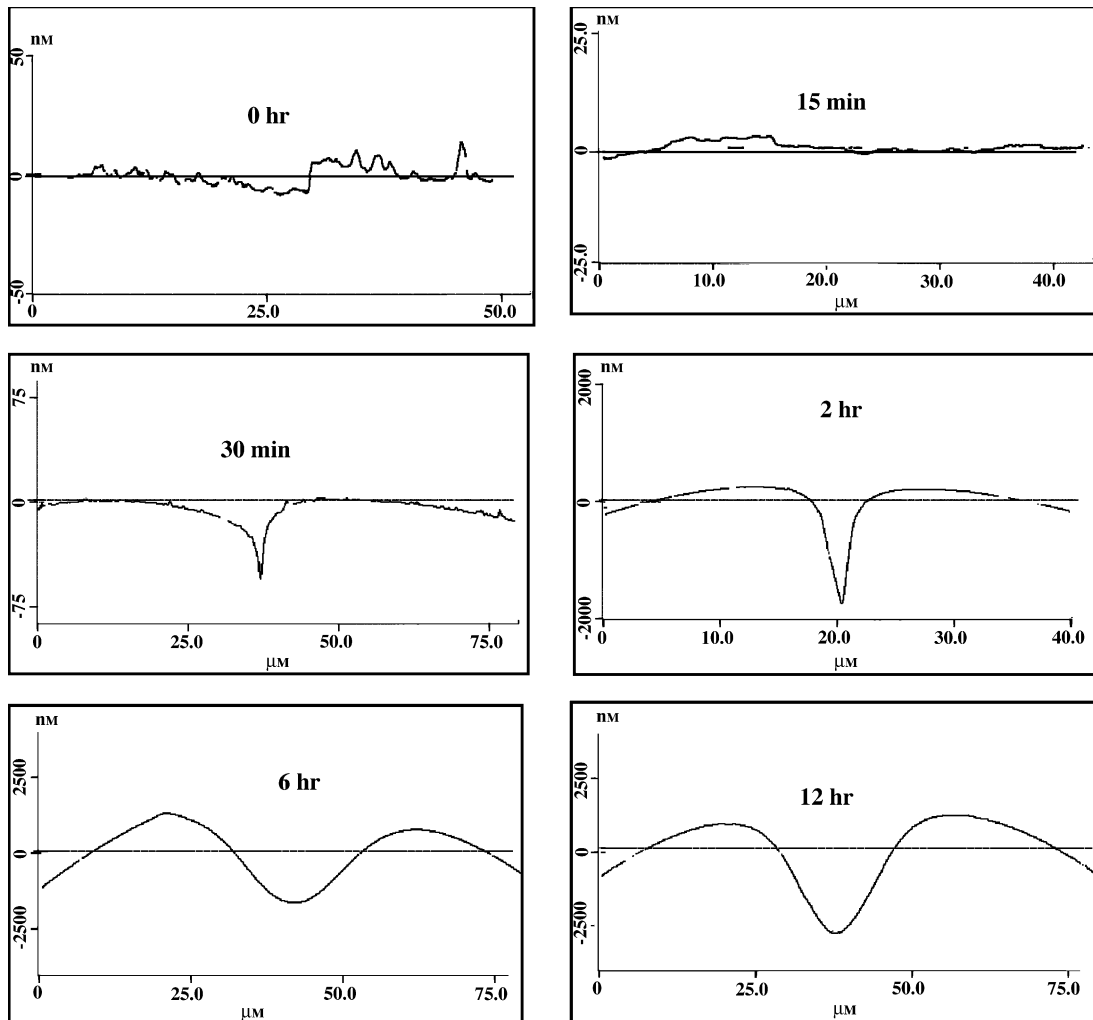


Fig. 3. Crack-tip profiles after annealing at various times at 630 °C.

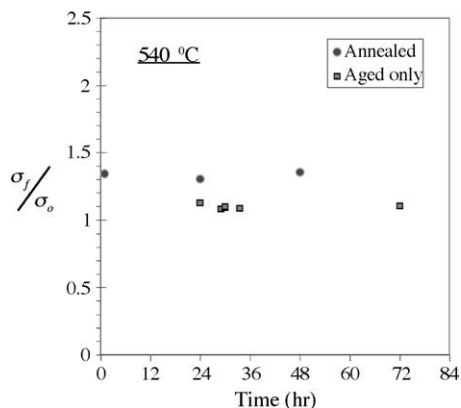


Fig. 5. Fracture strength as a function of annealing time at 540 °C. Also plotted are strength values of samples that had been aged only; for these results the time axis represents the length of time the sample aged between indentation and fracture-testing.

peratures, respectively. In both figures the fracture strength is normalised to the strength of the glass in the as-indent, no-ageing, no-annealing state, σ_o . The value of this reference strength was measured to be 15.02 MPa. Also plotted in Fig. 5 are the strength values obtained for specimens that had been fractured after ageing them for various lengths of time as explained in Section 2. For these results the time axis thus represents the length of time the samples aged between indentation and fracture testing. In Fig. 6 the same information is represented by the shaded bar that projects from the stress axis. These results show that once slow crack growth has reached saturation after ~ 24 h, no significant increase in strength will be obtained however long the residual contact system is aged. The normalised strength corresponding to this slow crack saturation is 1.1. This also means that ageing in air, which is accompanied by contact residual stress relaxation,^{4,5} results in a maximum increase in strength, relative to the as-indent state, of $\sim 10\%$. Salomonson et al.⁶ obtained 8.4%

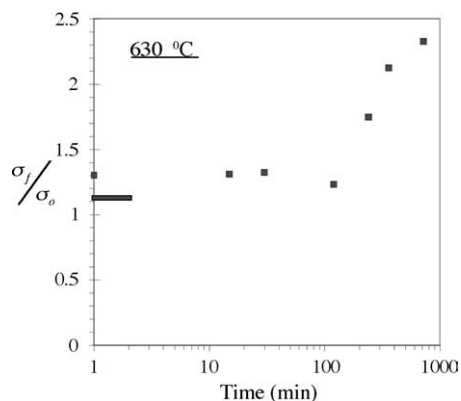


Fig. 6. Fracture strength as a function of annealing time at 630 °C. The shaded bar protruding from the vertical axis represents the value of strength obtained for samples that had been aged only after indentation, as explained in Fig. 5.

Table 3

Comparative results from Roach and Cooper⁵

Temperature	σ_f^{\max} (MPa)	σ_f^{\max}/σ_o
Room temperature	44	1.1
300 °C	47	1.18
400 °C	52	1.3
500 °C	52	1.3

$\sigma_o = 40$ MPa.

strength increase after ageing for 2 months. For further comparison with results from previous studies, Table 3 presents a summary of the relevant results of Roach and Cooper.⁵ In Table 3, σ_f^{\max} represents the saturation strength values at the conditions defined in the first column. σ_o has the same meaning as before.

The room temperature results of Cooper and Roach,⁵ Table 3, thus confirm our assertion above that the maximum strength increase to be obtained from slow crack growth is about 10%. Annealing, on the other hand, results in a larger relative strength increase. Our annealing study at 540 °C gave a strength increase of about 33% and, as may be seen in Fig. 5, this value is practically constant irrespective of the length of hold time at that annealing temperature. As shown in Table 3, Roach and Cooper⁵ virtually obtained the same limiting relative strength increase of 30% when samples were annealed at 400 and 500 °C for long hold times.

Up to 2 h hold time at 630 °C, practically the same constant relative increase in fracture strength of 30% is obtained, Fig. 6. Above 2 h anneal time at 630 °C the strength increases strongly with anneal time as may be seen in Fig. 6, where the strength increase reaches $\approx 132\%$ relative to the reference strength after annealing for 12 h.

The strength behaviour reported in Figs. 5 and 6 is of a similar form to that obtained by Hrma et al.¹⁰ (see Fig. 8 of ref.¹⁰) The main difference is that whereas their σ_f-t diagram is a composition of results obtained at different temperatures, here, we follow the strength development at each annealing temperature throughout the entire length of the experiment: 48 h at 540 °C and 12 h at 630 °C. As mentioned in Section 1, in this paper, we seek to relate the observed trends in strength to the progression of stress relaxation in the residual stress field. In contrast to the previous studies where the stress relaxation was measured as a representative optical retardation for the entire stress field,^{5,9} in the present study, the new method of stress estimation using nanoindentation¹¹ permits us to follow the relaxation profile across the entire stress field as annealing progresses. Fig. 7(a and b) are results obtained from ref.¹¹ showing stress relaxation as a function of annealing hold time in the Vickers residual stress field during constant temperature annealing at 540 and 630 °C. In Fig. 7, the distance x (μm), from the edge of the Vickers indent is normalised to half the length of the diagonal, $2d$. For a 45 N Vickers indent, $d \approx 61.5 \mu\text{m}$. The stress, σ , at any position, x , and time is normalised to the initial stress at that same position, x , before annealing started.

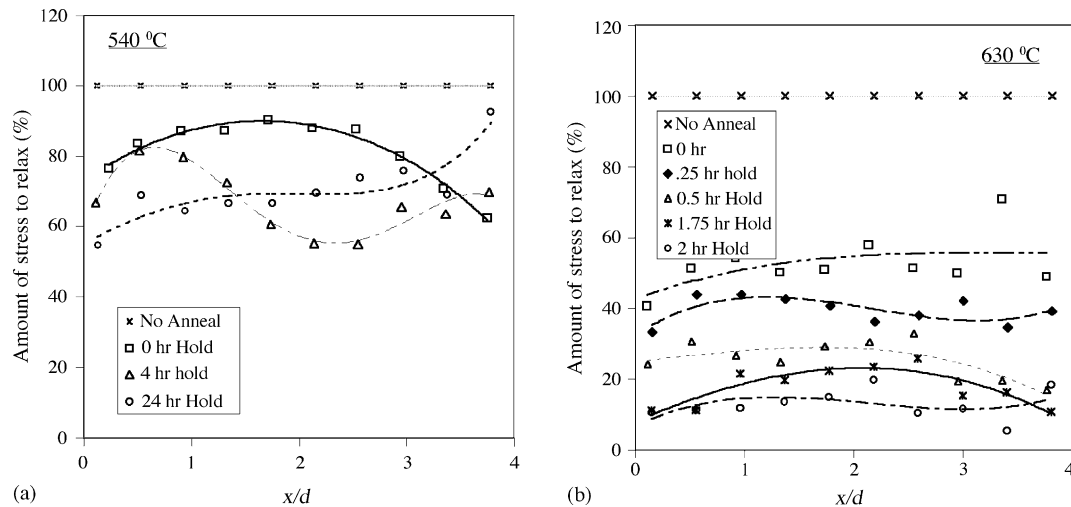


Fig. 7. Residual stress relaxation around a Vickers indent in soda-lime glass for (a) $T = 540\text{ }^{\circ}\text{C}$ ($<T_g$) and (b) $T = 630\text{ }^{\circ}\text{C}$ ($>T_g$).

3.2.1. Residual stress relaxation versus fracture strength

It can be seen from Fig. 7(a) that below T_g , stress relaxation rate is not very uniform across the stress field even if a general tendency for increased stress relief with time is evident. After annealing for 24 h however, the stresses seem to increase again from a distance of $\sim x = 1.5d$ and away from the indent. This resurgence of stress has also been measured by Solomonsson and Rowcliffe,²¹ who, using an indentation fracture method, discovered that after 24 h annealing at temperatures close to T_g , compressive stresses change sign and become tensile instead. This may therefore explain the crossover at $x = 1.5d$ in Fig. 7(a). The figure also shows that after 24 h, the stresses in the region of the field where the radial crack tips end ($x > 3.7d$), have increased almost to the initial value. Following Salomonson and Rowcliffe's results,²¹ this should mean increased tensile stresses, which should lead to a decrease in relative strength. This however is not the case in Fig. 5 where the fracture strength as mentioned before is constant irrespective of annealing hold time at $540\text{ }^{\circ}\text{C}$; neither does the strength increase if one, instead, were to attribute the stress resurgence to increasing compressive stresses. In other words, the trends in residual stress relaxation do not match strength behaviour measured after annealing at $540\text{ }^{\circ}\text{C}$. The issue is even better clarified by examining the experiment of $630\text{ }^{\circ}\text{C}$. Unlike the $540\text{ }^{\circ}\text{C}$ case, here, the relaxation is almost uniform everywhere in the residual stress field at each hold time, Fig. 7(b). Moreover, at the higher temperature, there is no significant stress resurgence and the stress is progressively relaxed with time throughout the stress field. The reason behind the different relaxation profiles for 540 and $630\text{ }^{\circ}\text{C}$, as explained in,¹¹ can be attributed to the difference in the kinetics of the plastic zone transformation processes at work on either side of the transformation temperature. The results of Fig. 6 show that, unlike stress relaxation, fracture strength does not increase progressively with annealing hold time but rather remains constant throughout the first 2 h of annealing. Just heating the sample up to $630\text{ }^{\circ}\text{C}$ and cooling

down to room temperature with zero time hold, for instance, results in between 50 and 60% stress relaxation throughout the stress field. The corresponding strength increase for the same annealing treatment, on the other hand, is only $\sim 30\%$. After 2 h annealing at $630\text{ }^{\circ}\text{C}$, the stresses (i.e. $\sim 90\%$ of the original stresses) are practically relieved around the Vickers indent. Yet the strength recovery after this period is only the same 30% as was obtained at lower anneal hold times. The conclusions from these analyses are that high temperature annealing indeed causes stress relaxation around the Vickers indent in glass. However, the stresses released during annealing are not necessarily converted to restored strength of the material. The part of the stress relaxation that impacts on the fracture strength properties occurs probably already during the heating up process, at much lower temperatures, and could even be transient in nature. This part results in a maximum strength increase of $\sim 30\%$. When this has occurred, practically no strength recovery is likely to be extracted from annealing unless changes in crack morphology occur. Han et al.⁹ and Hirao and Tomozawa²² also came to a similar conclusion, who observed that the effect of the contact residual stress on the strength was minimal.

3.2.2. Strength recovery beyond residual stress relaxation

In this sub-section we take a closer look at the results obtained here at $630\text{ }^{\circ}\text{C}$ for annealing times exceeding 2 h. As may be seen in Fig. 6 this region of annealing hold times is characterised by strong recovery of strength—up to 132% increase relative to the as-indented reference strength, after 12 h annealing. This region is beyond the stress relaxation phase since all stresses are essentially relieved after 2 h of annealing at that temperature. Thus, the strong recovery of strength here cannot be attributed to residual contact stress relaxation. Rather it could be due to the changes in crack morphology that occur there. It can be seen from Figs. 1–3 that strong crack tip rounding occurs in this region of marked

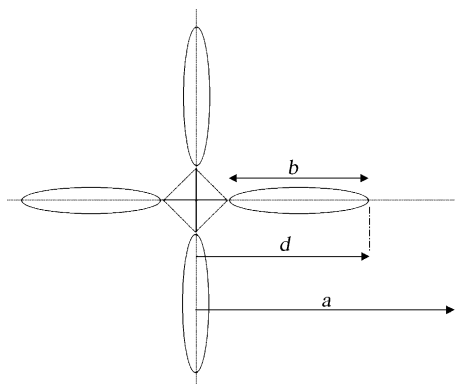


Fig. 8. A schematic representation of the Vickers indent-crack system showing changes in surface crack morphology after annealing at hold times exceeding 2 h at 630 °C. The changes include reduction of crack length and widening of crack opening. The rather faint outline of the edges of the indent are made to depict the real blurred appearance of the indent edge as a result of the high temperature viscous processes taking place.

strength recovery. Associated with this crack tip rounding is crack length shortening as can be seen for sample sets 8–10 in Table 2.

Fig. 8 is a typical representation of the indent/crack system beyond the stress relaxation phase, where reduction of crack length and widening of crack opening are illustrated. Let a be the crack length before annealing, then after a hold time exceeding 2 h at 630 °C, the tip of the crack at the surface has reached a point which is displaced d μm from the centre of the indentation. In Table 2 this is the crack length given for tests 8–10 under ‘crack length at fracture’. Fig. 8 also shows that crack pinch-off¹⁰ occurs at the zone of departure from the corners of the Vickers indent. This leads to the creation of another tip to the crack, resulting in what appears to be a complete surface segmentation of the original crack.

Thus, although fracture did originate from the site of the indent-crack system, the fracture-originating crack could be either b or d , as defined in Fig. 8. This is because, whereas a single crack extended on either side of each diagonal of the Vickers indent before annealing, it could be, after annealing, that these now are four separate cracks surrounding the indent.

This is illustrated in Fig. 9, which is a photomicrograph of a fracture surface containing the indent/crack system. The specimen had been annealed for 4 h at 630 °C. The solid arrow shows the trace of the initial radial/median crack system, while the dashed arrow shows the site of the part of the radial/median crack front that had been healed. Thus subsurface changes to the crack front during annealing, together with those occurring at the surface, can lead to important crack morphological changes that can influence the strength properties of the glass. Fig. 9 shows that these changes can occur when long time annealing takes place at temperatures above T_g , where viscous flow becomes important for the crack healing process.

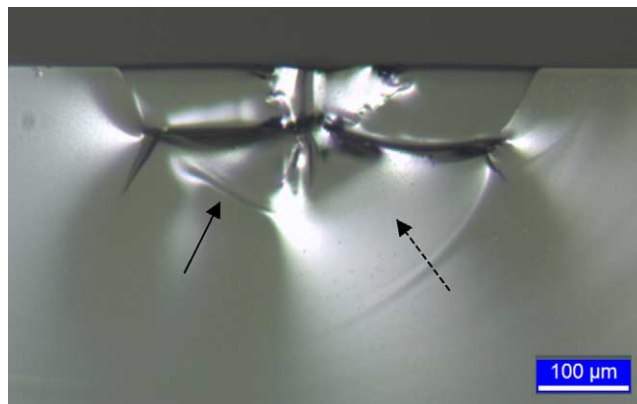


Fig. 9. Fracture surface of a 4 h anneal specimen showing the indent/crack site. Solid arrow shows radial/median crack front, while dashed arrow shows site of healed radial/median crack front.

3.3. Relating strength recovery to crack morphology changes

Comparison between Figs. 2 and 6 shows that crack tip radius varies with time in a way that is similar to the trend in fracture strength variation with time at 630 °C. That is, the fracture strength is practically constant in the region where the crack tip radius also does not change much; as the crack tip radius increases after 2 h hold time, the fracture strength also increases in a similar fashion. The fact that no crack growth occurred during the constant strength segments of Figs. 5 and 6 means that the stress relaxation that occurred through annealing did not involve crack growth unlike the relaxation caused by ageing (i.e. slow crack growth). This also means that contact residual stress relaxation at elevated temperatures does not necessarily translate into strength recovery of the material. The increase in strength at 540 °C and up to 2 h at 630 °C relative to that of the fully aged state thus corresponds to the residual stress relaxation that occurs before constant holding at these temperatures began, i.e. during the heating stage of the annealing cycle. (Note that the constant stress part at 630 °C has the same value of relative strength recovery as the 540 °C case.) Roach and Cooper⁵ obtained the same relative strength recovery values after annealing at 400 and 500 °C. It therefore appears that the contact residual stress has a component that influences strength. The temperature at which this begins to be rendered ineffective lies well below T_g . Once this has been passed, no strength recovery is to be gained from residual stress relaxation even though all the stresses are not yet completely relieved. Pajares et al.²³ came to a similar conclusion for 4 mol% yttria partially stabilised zirconia (4Y-PSZ), noting that even though residual stresses were not available to drive radial cracks after annealing at 1000 °C, that did not mean that the stresses were completely eliminated around the Vickers indent.

Thus, beyond the regime of influence of the contact residual stresses, the similarity in shape between the $\rho-t$ and the σ_f/σ_o-t plots suggests a correlation between the crack tip radius and the fracture strength. Although results of some

of the previous studies²⁴ of the subject have suggested a connection between strength increase and crack tip blunting, it is the present study that thus provides the experimental evidence of the correlation, through physical measurement of the crack tip as made possible by the AFM. On the discussion regarding sharpness or bluntness of the indentation crack tip^{4,5,24} the results of the present study lead us to conclude that (i) in the regime defined by room temperature ageing and the heating segment of an annealing cycle, the observed strength increase can be attributed to the release of residual stress that occurs, as described by Lawn et al.,⁴ (ii) beyond this regime, crack morphology changes take place, whose nature are such as to influence the fracture mechanics through crack healing, and by making the crack tip radius now important, as was suggested by Tomozawa et al.²⁴ In this connection, Kurkjian²⁵ suggested a modification of the Griffith equation to include the crack tip. Such an exercise was carried out in the present study using the experimentally measured tip radius, but the resulting plot varied much, in relative quantitative terms, from the experimental plot of Fig. 6.

3.3.1. Ultimate strength recovery

Once a sample is indented, it is not likely that ultimate strength recovery, corresponding to the as-received, unindented material can be achieved in practice since, as reported by Hrma et al.,¹⁰ weakening will set in as flaws other than the contact system begin to constitute the fracture origin with prolonged annealing. Thus, if the aim is to produce a stress-free contact system, then this can be achieved through annealing at temperatures exceeding T_g . This would however be at the cost of changed crack morphology, especially when prolonged annealing hold times are used at those temperatures. At temperatures below T_g , the system would behave as if no contact residual stresses were present even though all the stresses would not have been relieved. This explains the success of using the ‘stress-free’ annealed samples in the analyses by earlier workers (see for example⁴ and⁸). After annealing at those temperatures, a significant proportion of the original stresses remain around the Vickers indent, but as already explained, they do not influence the strength properties of the material. On the other hand, if the aim is to render contact flaws harmless in a bid to strengthen a product, then extended (but not prolonged) annealing at temperatures above T_g would be needed.

4. Conclusions

Strength recovery of soda lime glass after indentation may be divided into two regimes. (i) That of the first regime is characterised by the contact residual stress factor, χ , which has a high value immediately after indentation but decreases as the residual stress field relaxes, accompanied by slow crack growth in humid environment. Under these conditions strength increase is about 10% relative to the immediate as-

indented state. During annealing at elevated temperatures the contact residual stress factor decreases further, resulting in a further increase in relative strength. The relative strength increase at this stage is about 30%. It appears, from the present study, that this stage could be transient and occur well below T_g . (ii) During the initial part of the second regime, there is still residual stress to be relieved, but its component, χ , that impacts on strength has become zero. For temperatures below T_g complete stress relaxation may take a very long time while the time may be relatively short at annealing temperatures above T_g . No increase in strength occurs during this initial part, until the stresses are completely relieved and clear crack morphological changes begin to occur. After 12 h at 630 °C for example the relative strength increase measured was about 132%.

The strength recovery trend in the second regime, beyond the influence of the contact residual stress factor, χ , has been experimentally shown to have a good correlation with the crack tip radius as a result of the crack tip blunting that occurs during annealing.

References

- Zeng, K. and Rowcliffe, D., Experimental measurement of residual stress field around a sharp indentation in glass. *J. Am. Ceram. Soc.*, 1994, **77**, 524–530.
- Chiang, S. S., Marshall, D. B. and Evans, A. G., The response of solids to elastic/plastic indentation. I. Stresses and residual stresses. *J. Appl. Phys.*, 1982, **53**, 298–311.
- Yoffe, E. H., Elastic stress fields caused by indenting brittle materials. *Philos. Mag. A*, 1982, **46**, 617–628.
- Lawn, B. R., Jakus, K. and Gonzalez, A. C., Sharp vs. blunt crack hypothesis in the strength of glass: A critical study using indentation flaws. *J. Am. Ceram. Soc.*, 1985, **68**, 25–34.
- Roach, D. H. and Cooper, A. R., Effect of contact residual stress relaxation on fracture strength of indented soda-lime glass. *J. Am. Ceram. Soc.*, 1985, **68**, 632–636.
- Salomonson, J., Zeng, K. and Rowcliffe, D., Decay of residual stress at indentation cracks during slow crack growth in soda-lime glass. *Acta Mater.*, 1996, **44**, 543–546.
- Abe, H., Ikeda, K., Nakashimu, H., Yoshida, F. and Koga, K., Evaluation of indentation induced residual stress in the surface of float glass. *J. Ceram. Soc. Jpn.*, 2000, **108**, 416–419.
- Marshall, D. B. and Lawn, B. R., Flaw characteristics in dynamic fracture: The influence of residual contact stresses. *J. Am. Ceram. Soc.*, 1980, **63**, 532–536.
- Han, W. T., Hrma, P. and Cooper, A. R., Residual stress decay of indentation cracks. *Phys. Chem. Glasses*, 1989, **30**, 30–33.
- Hrma, P., Han, W. T. and Cooper, A. R., Thermal healing of cracks in glass. *J. Non-Cryst. Solids*, 1988, **102**, 88–94.
- Kese, K., Tehler, M. and Bergman, B., Contact residual stress relaxation in soda lime glass. I. Measurement using nanoindentation. *J. Eur. Ceram. Soc.*, submitted for publication.
- Lange, F. F. and Gupta, T. K., Crack healing by heat treatment. *J. Am. Ceram. Soc.*, 1970, **53**, 54–55.
- Yen, C. F. and Coble, R. L., Spheroidization of tubular voids in Al_2O_3 crystals at high temperatures. *J. Am. Ceram. Soc.*, 1972, **55**, 507–509.
- Gupta, T. K., Crack healing in thermally shocked MgO. *J. Am. Ceram. Soc.*, 1975, **58**, 143.
- Gupta, T. K., Crack healing and strengthening of thermally shocked alumina. *J. Am. Ceram. Soc.*, 1976, **59**, 259–262.

16. Evans, A. G. and Charles, E. A., Strength recovery by diffusive crack healing. *Acta Metall.*, 1977, **25**, 919–927.
17. Lehman, R. L., Hill Jr., R. E. and Sigel, G. H., Low-temperature crack closure in fluoride glass. *J. Am. Ceram. Soc.*, 1989, **72**, 474–477.
18. Holden, M. K. C. and Frechette, V. D., Healing of glass in humid environments. *J. Am. Ceram. Soc.*, 1989, **72**, 2189–2193.
19. Wilson, B. A. and Case, E. D., In situ microscopy of crack healing in borosilicate glass. *J. Mater. Sci.*, 1997, **32**, 3163–3175.
20. Ackler, H. D., Healing of lithographically introduced cracks in glass and glass-containing ceramics. *J. Am. Ceram. Soc.*, 1998, **81**, 3093–3103.
21. Salomonson, J., *Indentation Fracture of Alumina and Glass*. PhD thesis, Royal Institute of Technology, Stockholm, Sweden, 1996.
22. Hirao, K. and Tomozawa, M., Kinetics of crack tip blunting of glasses. *J. Am. Ceram. Soc.*, 1987, **70**, 43–48.
23. Pajares, A., Guiberteau, F., Steinbrech, R. W. and Dominquez-Rodriguez, A., Residual stresses around Vickers indents. *Acta Metal. Mater.*, 1995, **43**, 3649–3659.
24. Tomozawa, M., Hirao, K. and Bean, P. E., Origin of strength increase of abraded or indented glass upon annealing. *J. Amer. Ceram. Soc.*, 1986, **69**, C-186–8.
25. Kurkjian, C. R., Mechanical stability of oxide glasses. *J. Non-Cryst. Solids*, 1988, **102**, 71–81.